Asian Journal of Chemistry; Vol. 38, No. 5 (2026), 1177-1188

ASIAN JOURNAL OF CHEMISTRY

https://doi.org/10.14233/ajchem.2026.35477

Mustard Waste-Derived Activated Carbon for Efficient Removal of Malachite Green from Aqueous Solution

POOJA MEENA, REKHA SHARMA, ASHISH DEV KANWADIA, POOJA and BHANUPRIYA MORDHIYA*

Department of Chemistry, University of Rajasthan, Jaipur-302004, India

*Corresponding author: E-mail: bmordhiya@gmail.com

Received: 17 December 2025 *Accepted*: 13 March 2026 *Published online*: 4 May 2026 AJC-22342

This study demonstrates the effective use of mustard-waste-derived activated carbon as a sustainable and low-cost adsorbent for the removal of malachite green dye from aqueous solutions. SEM and TEM analyses revealed a highly porous and heterogeneous surface, while FTIR confirmed the presence of functional groups (-OH, -COOH, -C=O), facilitating dye adsorption. BET analysis yielded a surface area of 125.3 m^2/g with a monolayer adsorption volume (V_m) of 28.79 cm^3/g and a BET constant (C) of 43.34, indicating strong adsorbate-adsorbent interactions. Batch experiments achieved a maximum removal efficiency of 97.97% at pH 8, contact time of 80 min and adsorbent dose of 50 mg. Adsorption kinetics followed the pseudo-second-order model ($R^2 > 0.99$), suggesting chemisorption, while equilibrium data fitted the Langmuir isotherm ($R^2 = 0.987$) with a maximum capacity of 46.34 mg/g. Thermodynamic studies confirmed a spontaneous and endothermic adsorption process.

Keywords: Mustard waste, Adsorbent, Malachite green, Eco-friendly adsorbent, Langmuir isotherm.

INTRODUCTION

Synthetic dyes are widely used in printing, painting, food, textile and related industries. A significant portion of these dyes enters wastewater, with nearly 10% reaching aquatic environments during processing, causing serious pollution problems [1,2]. At high concentrations, many dyes are toxic and harmful to both humans and aquatic organisms. Conventional treatment methods such as precipitation, photodegradation and commercial activated carbon adsorption are often costly and may generate secondary waste [3,4]. Hence, efficient and low-cost alternatives are needed. Activated carbon is a highly effective adsorbent due to its porous structure, large surface area, and strong adsorption capacity, making it widely used for wastewater treatment [5-7].

Among the available approaches, the use of agricultural waste materials as low-cost biosorbents has gained significant attention since they are abundant, renewable and rich in functional groups capable of binding dye molecules [8,9]. In this context, mustard waste is particularly attractive. Rajasthan, one of India's major mustard-producing states, generates large amounts of mustard residues after harvesting. These residues, mainly stalks and husks, are lignocellulosic in nature and contain lignin along with surface hydroxyl and carboxyl groups that provide strong adsorption potential for dye removal [10]. Their utilization can also reduce the environmental burden caused by open disposal or burning of crop residues. In granular form, mustard waste has shown promise in wastewater filtration and adsorption processes [11-13]. Furthermore, the glucosinolate content of mustard residues limits their use as animal feed, making valorisation as an adsorbent more practical [14]. Similar plant-based wastes such as banana peel, rice husk, sawdust, orange peel and sugarcane bagasse have also demonstrated effective malachite green removal due to their porous lignocellulosic structure and reactive functional groups [15-17].

Malachite green is extensively used for colouring silk, leather and paper, and as an antifungal agent in aquaculture. However, its non-biodegradable, toxic and potentially carcinogenic nature makes it a hazardous aquatic pollutant, highlighting the urgent need for efficient wastewater treatment methods [18-20]. Limited research has examined the use of mustard crop residue for malachite green adsorption. This study aims to explore the potential of mustard crop residue as a low-cost biosorbent for removing malachite green from aqueous solutions. The research will focus on characterizing the biosorbent, evaluating the adsorption performance under varying conditions and analyzing the adsorption isotherms and kinetics.

EXPERIMENTAL

The chemicals used throughout the experiment were of analytical grade and obtained from Loba Chemie Pvt. Ltd., India including malachite green dye ($C_{23}H_{25}ClN_2$), sodium hydroxide, potassium hydroxide, hydrochloric acid, ethyl alcohol and other reagents for pH adjustment. A 1000 mg/L stock solution of malachite green dye was prepared in double-distilled water and diluted to the desired concentrations for further experimentation.

Mustard waste (crop residue): Mustard (*Brassica nigra*) crop residues were collected from local agricultural fields in the village of Karauli district (26.4934º N, 77.1035º E), Rajasthan, India. The raw biomass was thoroughly washed with tap water followed by distilled water to remove dirt, dust and surface impurities. It was then pulverized using a mechanical grinder, sieved to obtain a uniform particle size (100-250 μm) and dried in a hot air oven at 80 ºC for 24 h. The prepared biomass was finally stored in airtight containers for further use.

Preparation of modified adsorbent from mustard waste: The dried mustard residue was carbonized in a muffle furnace at 400 ºC for 1 h. The obtained char was chemically activated with KOH using a 1:2 weight ratio (char:KOH), followed by heating at 80 ºC for 12 h to ensure complete impregnation. The activated material was then reheated at 400 ºC for 1 h to complete the activation process. Finally, the product was mechanically ground into a fine powder and stored in airtight containers for subsequent adsorption studies.

Characterization: X-ray diffraction (XRD) analysis was carried out across a 2θ range of 10º to 80º using a PANalytical XPERT PRO diffractometer equipped with Cu*K*α radiation, running at 40 kV and 40 mA, to assess the crystallinity, structural purity and crystallite size of the synthesised materials. Using a Nova Nano FESEM-450 (FEI) for scanning electron microscopy (SEM) and high-resolution transmission electron microscopy (HRTEM), the surface morphology, particle sizes and microstructural features were investigated. Energy-dispersive spectroscopy (EDS) was employed to determine the elemental composition of the samples. Fourier transform infrared (FTIR) spectra were recorded on a Perkin-Elmer FTIR spectrometer in the range of 4000-400 cm^{-1} to identify the functional groups and bonding characteristics. Brunauer-Emmett-Teller (BET) analysis was carried out using a NOVA Touch 2LX surface area analyzer to evaluate specific surface area, pore size, pore volume, pore type and pore distribution.

Adsorption experiments: Batch adsorption studies were conducted to evaluate the dye-removal efficiency of the prepared activated carbon. Experiments were carried out in 250 mL conical flasks containing 50 mL of malachite green dye solution under varying pH (2-10) and contact time (10-100 min). The adsor-bent dosage was 0.02-0.05 g, the initial dye concentration was 10-60 mg/L and the temperature was 20-60 ºC. The pH was adjusted with 0.1 N HCl or NaOH. All flasks were agitated on a magnetic stirrer at 150 rpm. After the designated time, samples were filtered and analysed spectrophotometrically at 617 nm to determine the remaining malachite green dye concentration:

$$q_e = \left(\frac{C_o - C_e}{m}\right) \times V \quad (1)$$

$$q_t = \left(\frac{C_o - C_t}{m}\right) \times V \quad (2)$$

Using standard eqns. 1 and 2, the adsorption capacity (q_e) and percentage removal, respectively were calculated. The obtained results were further analysed using isotherm, kinetic and thermodynamic models to better understand the adsorption behaviour of malachite green onto mustard waste-derived activated carbon.

Statistical analysis: All adsorption experiments were conducted in duplicate and the average values were reported for reliability. Only small differences were observed between replicate measurements, indicating good consistency of the experimental procedure. Where required, the error bars showing standard deviation were included in the adsorption plots to represent experimental uncertainty.

RESULTS AND DISCUSSION

XRD studies: The X-ray diffraction (XRD) pattern of the mustard waste-derived adsorbent (Fig. 1) shows a broad peak in the 2θ range of 15º-30º, indicating the predominantly amorphous nature of the material. Such diffuse peaks are the characteristic of non-crystalline carbon structures commonly observed in biomass-derived activated carbons. The absence of sharp diffraction peaks confirms the lack of long-range crystalline order, which is typical for lignocellulosic carbon materials [21]. A weak peak near 2θ = 29.5º is assigned to the (002) plane of graphitic carbon in a disordered or turbostratic form. Similar patterns have been reported for activated carbons prepared from agricultural wastes such as coconut shell and rice husk [22-24]. The amorphous structure is beneficial for adsorption since it provides irregular pores, surface defects, and heterogeneous active sites that enhance dye uptake. The disordered carbon framework also contributes to higher surface

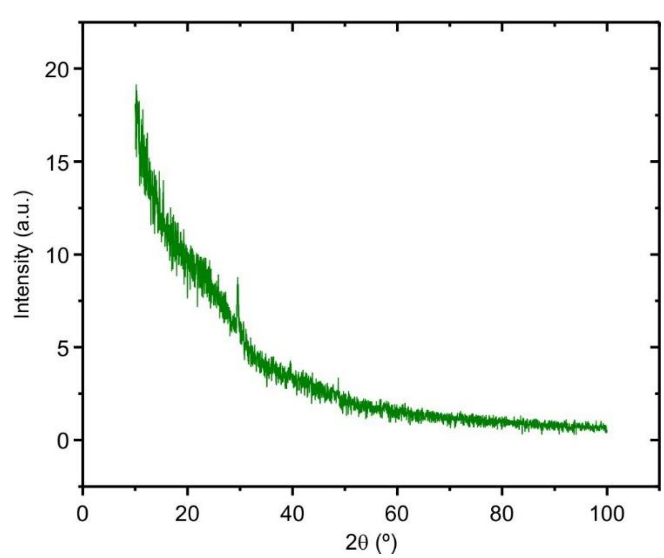

Fig. 1. XRD spectrum of mustard waste derived adsorbent

reactivity. These results confirm that the mustard waste-derived adsorbent possesses structural features favourable for efficient adsorption applications.

FT-IR studies: The FTIR spectrum of mustard waste-derived activated carbon reveals several characteristic absorption bands, confirming the presence of surface functional groups key for adsorption (Fig. 2). A broad band centered at 3424 cm^{-1} is assigned to O–H stretching vibrations of hydroxyl groups and adsorbed moisture, commonly observed in biomass-derived carbons and likely related to residual lignocellulosic constituents. Peaks at 2924 and 2853 cm^{-1} correspond to aliphatic C–H stretching of $-CH_2$ and $-CH_3$ groups, indicating partial retention of the organic carbon framework after carbonization [25]. The absorption band at 2344 cm^{-1} is attributed to physically adsorbed CO_2 (asymmetric stretching mode) on the porous surface. A distinct peak near 1623 cm^{-1} arises from C=C stretching vibrations of aromatic domains, suggesting the development of conjugated carbon structures and partial graphitization within the carbon matrix [26]. The band at 1404 cm^{-1} is associated with C–O stretching or O–H bending vibrations, indicating oxygen-containing functionalities such as phenolic or carboxylic groups on the surface [27]. The peaks in the 1100-1000 cm^{-1} region are assigned to C–O stretching vibrations of alcohol, ether or ester groups [28], while weaker absorptions between 800-500 cm^{-1} correspond to the out-of-plane bending of aromatic C–H bonds. The presence of hydroxyl, oxygenated and aromatic surface groups indicates multiple active sites capable of electrostatic interaction, hydrogen bonding and π-π interactions with malachite green molecules, thereby enhancing adsorption performance [29].

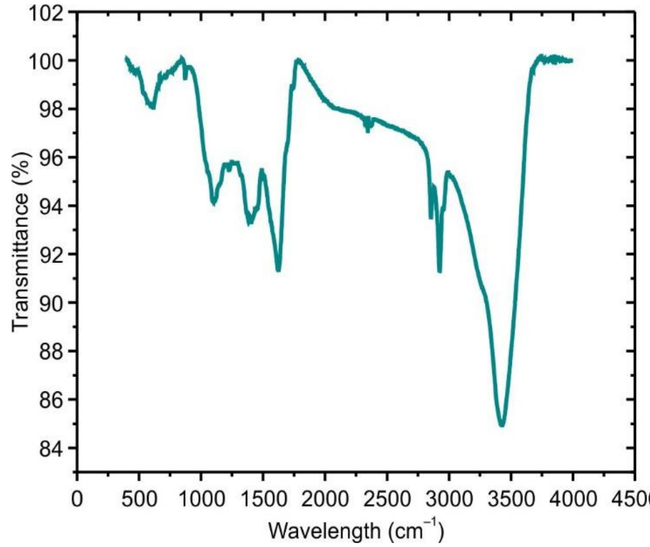

Fig. 2. FTIR spectrum of the adsorbent obtained from mustard waste

Surface morphology studies (SEM): The SEM micrographs of mustard waste-derived activated carbon reveal a highly porous and irregular surface morphology, which is a desirable characteristic for efficient adsorbents (Fig. 3). At

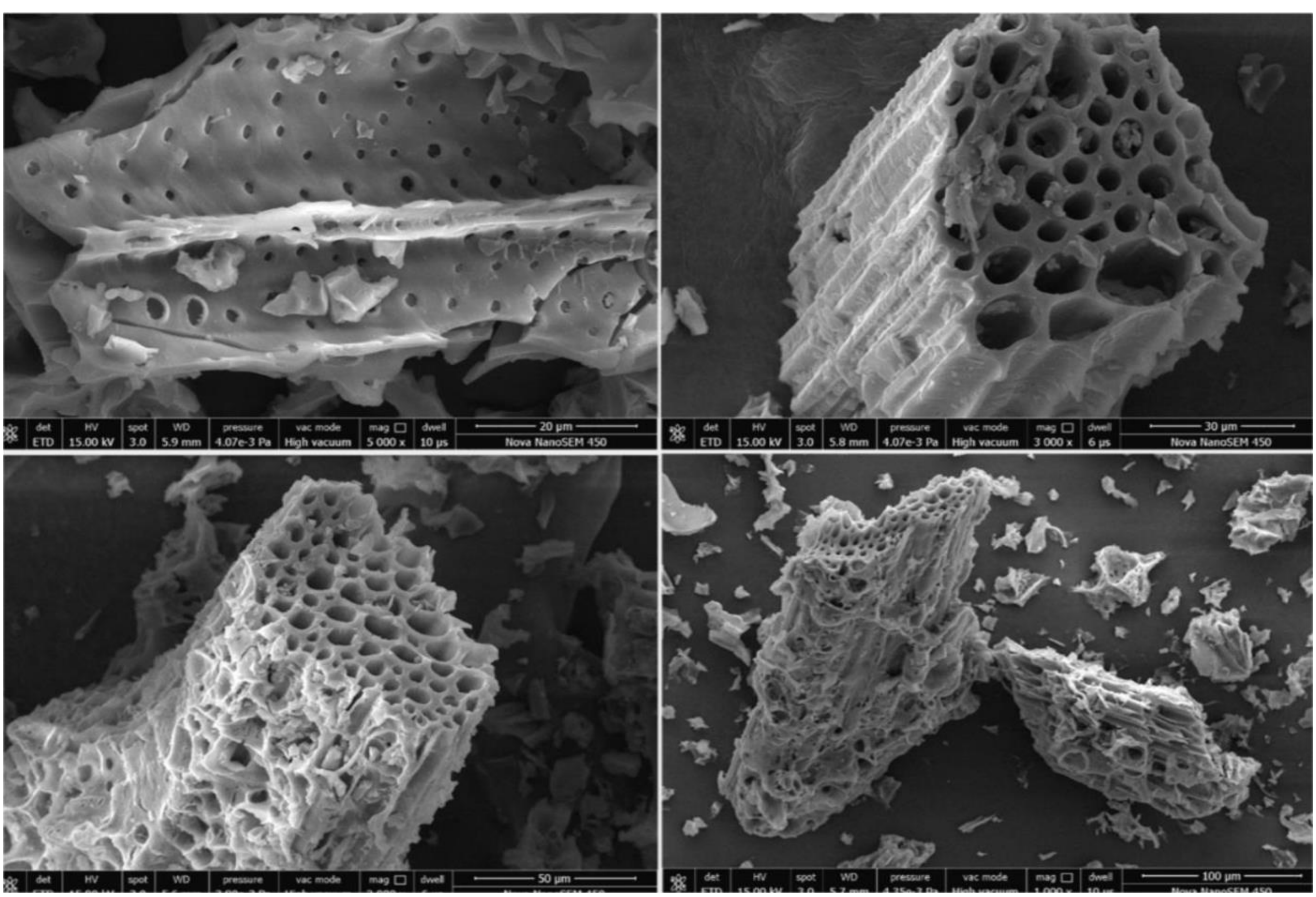

Fig. 3. SEM micrographs of activated carbon obtained from mustard waste

different magnifications, the images show a well-developed pore network with cavities of varying shapes and sizes, indicating the coexistence of micro- and mesoporous structures [30]. The sponge-like and honeycomb-like texture observed in several regions suggests effective carbonization and chemical activation, resulting in increased surface roughness and pore development.

The fractured and layered surface features with exposed internal voids are also visible, confirming the decomposition of lignocellulosic constituents and the removal of volatile components during thermal treatment [31,32]. Such textural modifications significantly enhance the accessible surface area and provide more active sites for adsorption of dye molecules such as malachite green. The interconnected pore channels are expected to facilitate rapid mass transfer and improved diffusion of pollutants into the adsorbent matrix. Irregular and sharp-edged particles observed in some areas may be attributed to structural etching caused by KOH activation. These observations confirm the formation of a heterogeneous porous carbon material suitable for wastewater treatment applications [33].

EDS analysis (Fig. 4) further confirmed that carbon is the dominant element, verifying successful formation of a carbon rich adsorbent. The presence of oxygen indicates surface oxygenated functional groups that can promote adsorption through hydrogen bonding and electrostatic interactions. Minor

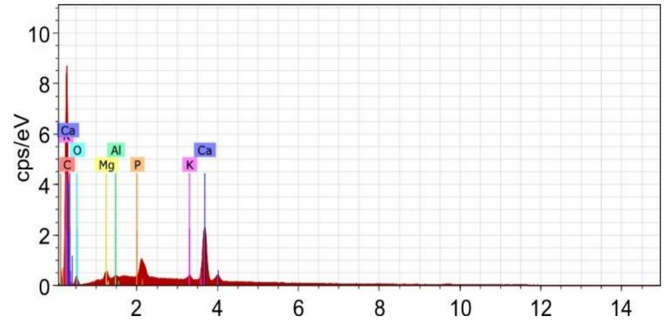

Fig. 4. EDS spectrum of activated carbon prepared from mustard waste

amounts of calcium, magnesium, potassium, phosphorus and aluminium were also detected, originating likely from the natural mineral content of mustard biomass or residual activation byproducts.

TEM studies: TEM images at varying magnifications were obtained to study the surface morphology of the synthesised activated carbon (Fig. 5a-e). At the lowest magnification (Fig. 5a, 200 nm), particles appeared as irregular agglomerates with heterogeneous contrast, indicating differences in thickness and density. As magnification increased to 100 nm (Fig. 5b), the aggregated particles exhibited a porous, loosely packed structure, suggesting interconnected nanostructures. Higher magnification (Fig. 5c, 50 nm; Fig. 5d, 20 nm) revealed finer features, with nano-sized domains featuring

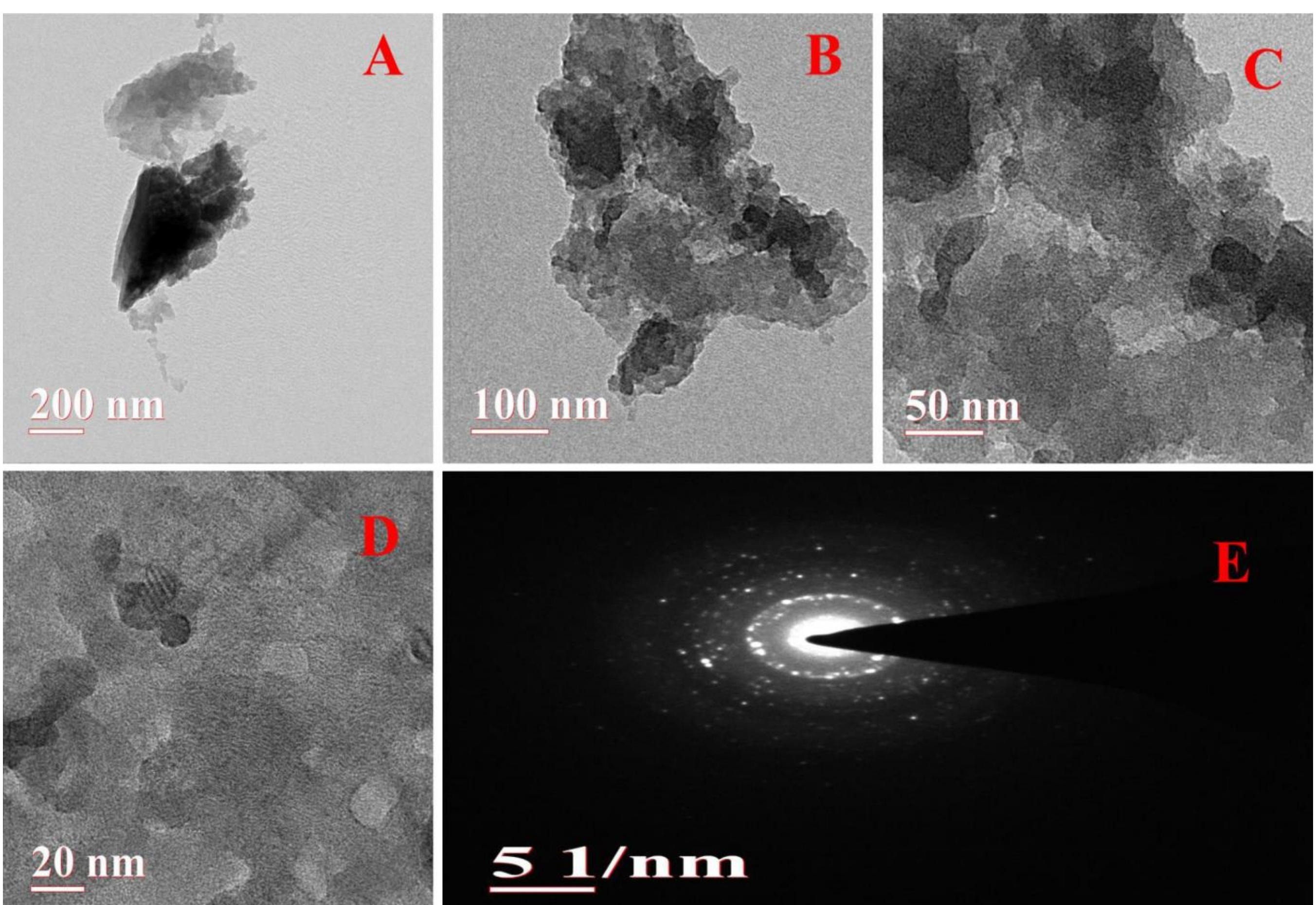

Fig. 5. TEM micrographs of the prepared adsorbent at different magnifications: (A) 200 nm, (B) 100 nm, (C) 50 nm, (D) 20 nm and (E) 5 nm

rough surfaces. Lattice fringes in Fig. 5d confirm some regions are crystalline, while amorphous areas point to a partially crystalline structure. The SAED pattern (Fig. 5e) displayed concentric rings with bright spots, confirming the material's polycrystalline nature. The coexistence of crystalline and amorphous regions indicates both ordered and disordered structures in the nanomaterial. This porous, polycrystalline morphology benefits adsorption and catalytic applications by offering a high surface area and numerous active sites for interaction [34].

BET studies: The Brunauer-Emmett-Teller (BET) analysis was carried out to evaluate the specific surface area and textural properties of mustard waste-derived adsorbent. The nitrogen adsorption-desorption isotherm exhibited a typical Type IV curve with an H3 hysteresis loop, characteristic of mesoporous materials with slit-shaped pores. The BET plot was constructed within the relative pressure range of 0.30-0.05, showing good linearity, validating the applicability of the BET model. The calculated monolayer adsorption volume (V_m) was 28.79 cm^3/g (STP), with a corresponding BET constant (C) of 43.34, indicating favourable adsorbate-adsorbent interactions and a uniform energy distribution of adsorption sites (Fig. 6). Using the molecular cross-sectional area of nitrogen (0.162 nm^2), the BET surface area was determined to be 125.3 m^2/g. Furthermore, the total pore volume (V_t) was estimated to be 0.128 cm^3/g, while the average pore diameter was calculated as 4.10 nm, confirming the predominance of mesoporous structures. The moderate surface area, coupled with well-developed mesoporosity, provides abundant active sites and efficient diffusion pathways for dye molecules. These findings demonstrate that the mustard waste can be effectively converted into activated carbon with promising adsorption characteristics, making it a sustainable and low-cost biosorbent for wastewater treatment applications [35,36].

Batch adsorption studies

Effect of contact time: The adsorption of malachite green onto mustard waste-derived activated carbon is strongly influenced by contact time at different concentrations (10-60 mg/L), with a dose amount of 40 mg. As shown in Fig. 7, a

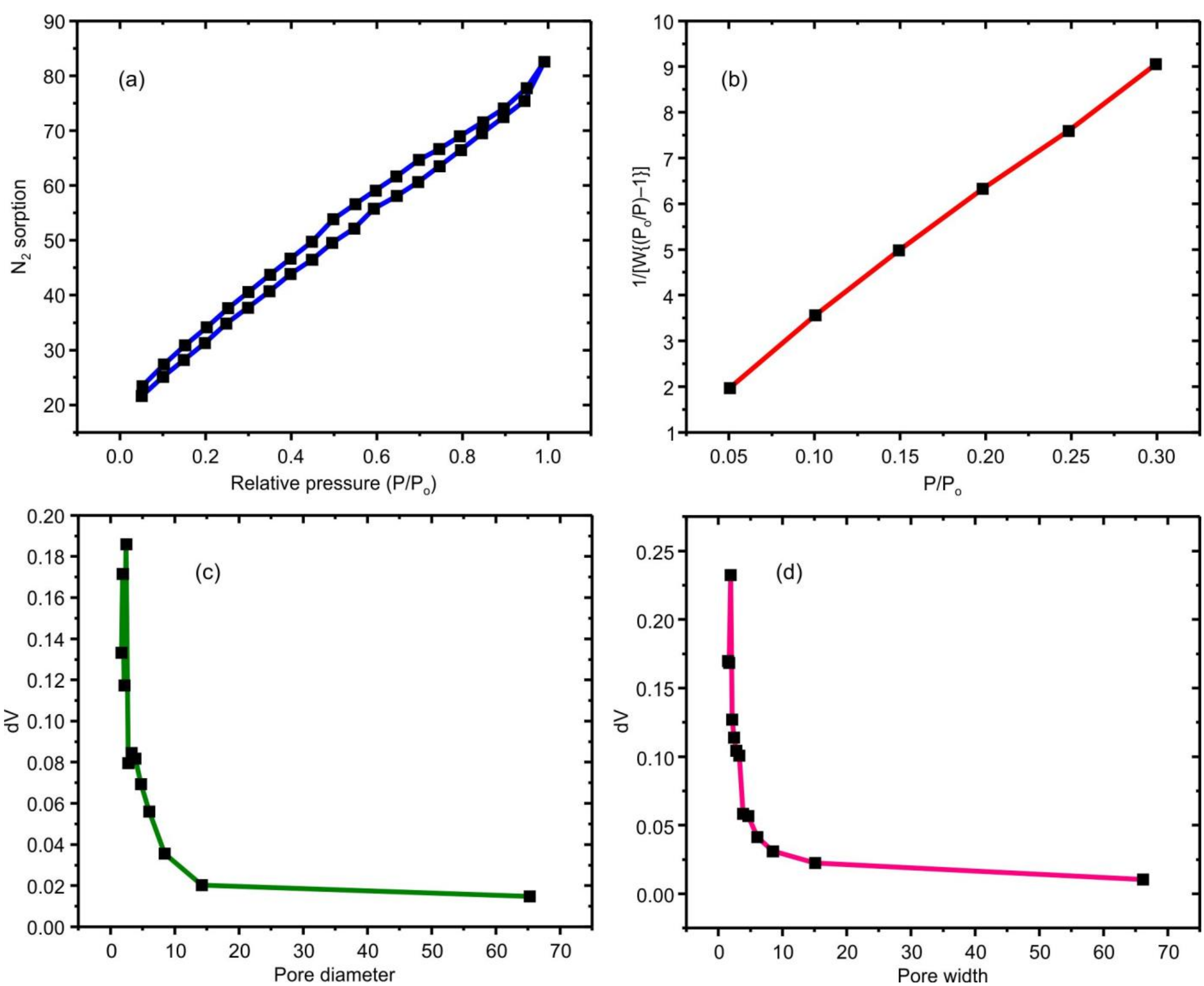

Fig. 6. (a) N_2 adsorption-desorption isotherm, (b) BET surface area analysis and (c,d) BJH pore size distribution of mustard waste derived activated carbon

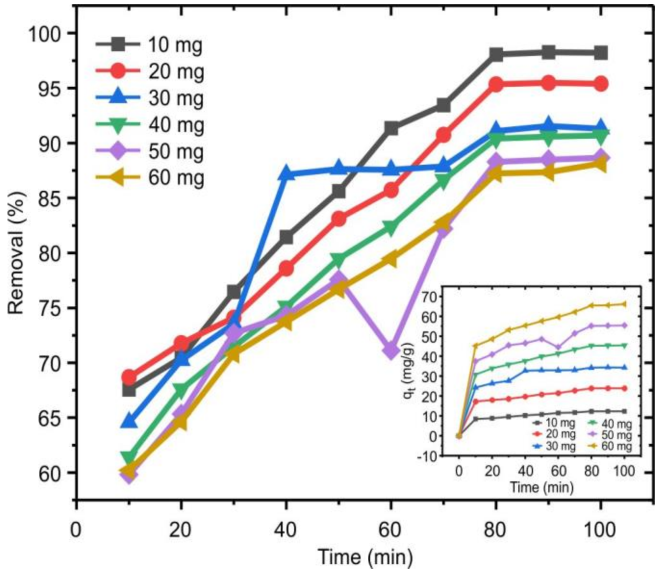

Fig. 7. Adsorptive performance of mustard waste derived activated carbon toward malachite green dye at different contact times

rapid increase in removal efficiency was observed during the first stage of adsorption, attributed to the abundance of readily available surface-active sites. As time progressed, the adsorption rate gradually decreased, reaching equilibrium once most of the active sites were occupied. At equilibrium, the removal efficiency was 98.05% at a contact time of 80 min. Interestingly, the corresponding adsorption capacity (q_t) increases from 24.5 to 127.5 mg/g as the concentration increases. This indicates that although the adsorbent showed a slightly lower removal percentage at higher dye concentrations due to the saturation of available active sites, the adsorption capacity increased markedly as a result of the stronger concentration gradient and enhanced mass transfer driving force at elevated concentrations [37].

Effect of pH: As shown in Fig. 8a, at lower pH 2-4, the percentage removal of the dye was relatively low due to the excess concentration of H^+ ions, which compete with the cationic malachite green molecules for available active sites on the adsorbent surface. As pH increased, the adsorption efficiency improved significantly, reaching a maximum of 97.97% at pH 8. This enhancement can be attributed to the increased negative charge on the adsorbent surface at higher pH, which strengthens the electrostatic attraction between the cationic dye molecules and the adsorbent. However, a slight decrease in removal efficiency was observed at pH 10, likely due to dye precipitation or alterations in surface chemistry under highly alkaline conditions [38,39]. These findings indicate that optimal malachite green adsorption occurs at pH 8, where the electrostatic interactions are most favourable.

Effect of temperature: The influence of temperature on the adsorption of malachite green dye onto mustard waste-derived activated carbon was studied in the range of 293.15-333.15 K. As shown in Fig. 8b, the adsorption efficiency increases with temperature. At 293.15 K (20 ºC), the removal efficiency was 97.98%, rising to 98.35% at 303.15 K (30 ºC). A more pronounced improvement was observed at 333.15 K (60 ºC), where dye removal reached 98.43%. This increase in adsorption capacity with rising temperature suggests that the process is endothermic. The higher temperature likely promotes greater mobility of malachite green dye molecules and enhances their interaction with the available active sites on the adsorbent surface [40,41].

Effect of adsorbent amount: The influence of the adsorbent dose on dye removal efficiency is presented in Fig. 9a. A gradual increase in removal efficiency was observed as the adsorbent dosage increased from 0.02 to 0.05 g. At the lowest dose of 0.02 g, the removal efficiency was approximately 59.90%, which steadily increased to 73% at 0.03 g. A significant enhancement was observed at 0.04 g, where the removal efficiency reached 90.17% and further increased to 0.05 g, achieving nearly complete removal. The improvement in performance with increasing adsorbent dose can be attributed to the greater availability of active adsorption sites [42]. The removal efficiency increased with increasing adsorbent dose due to the greater availability of active sites. However, beyond a certain dosage, the improvement became marginal, possibly due to particle aggregation and overlapp-

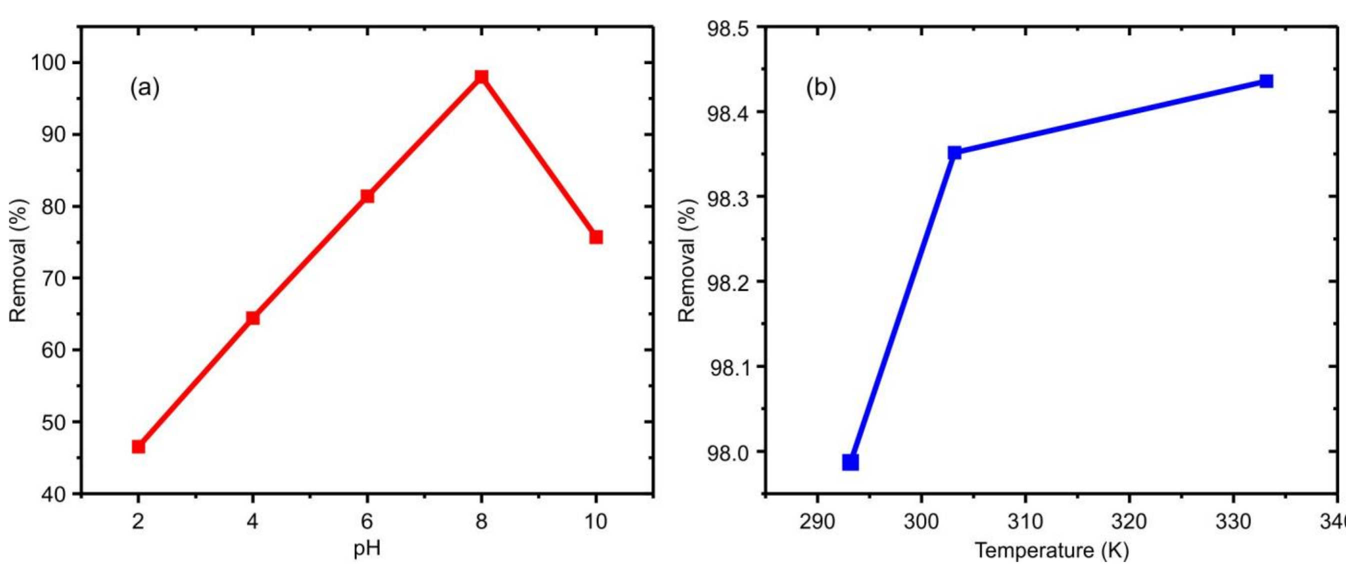

Fig. 8. Effect of (a) solution pH and (b) temperature on the adsorption of malachite green dye onto mustard waste-derived adsorbent

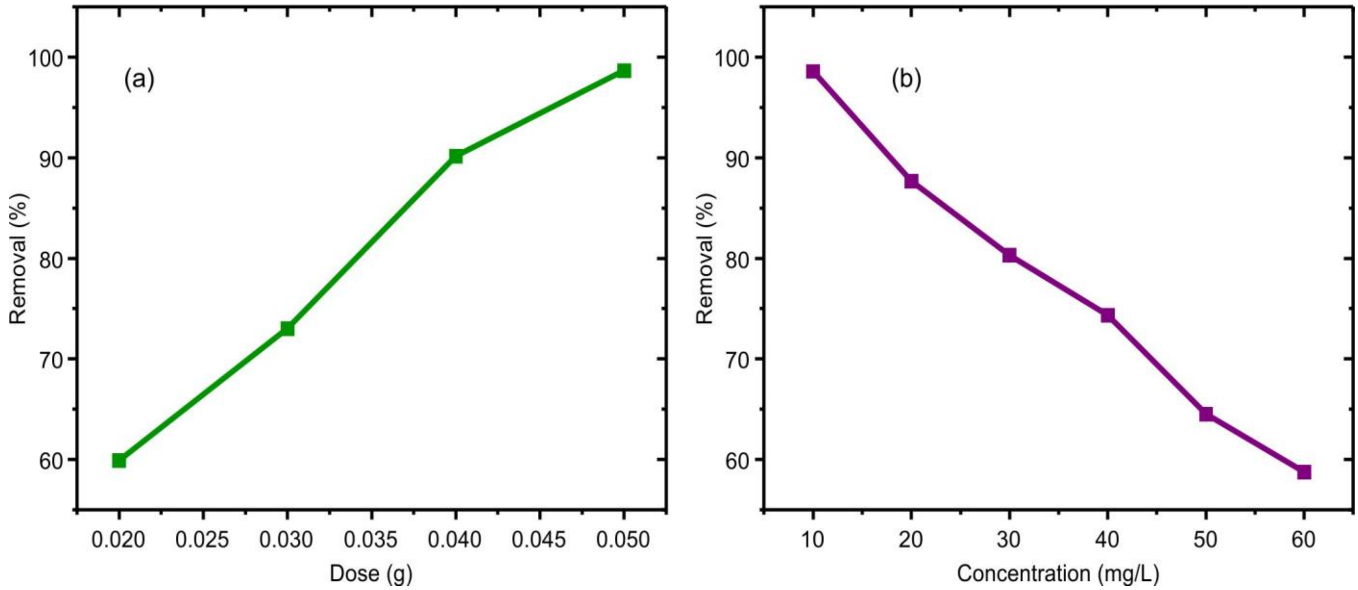

Fig. 9. Effect of (a) dose amount (b) initial dye concentration on the adsorption of malachite green dye onto mustard waste derived activated carbon

ing adsorption sites. Therefore, 0.05 g was selected as the optimum dose for the subsequent experiments.

Effect of varying initial dye concentrations: Fig. 9b shows the effect of the initial malachite green concentration on its removal by mustard waste-derived activated carbon. The removal efficiency decreased as the dye concentration increased from 10 to 60 mg/L. At 10 mg/L, the adsorbent exhibited a 98.59% removal efficiency, primarily due to the large number of accessible adsorption sites relative to the dye molecules. However, as concentration increased, the percentage removal declined to 58.73% at 60 mg/L, which can be attributed to saturation of adsorption sites and limited binding capacity at higher solute loads. Although efficiency decreases with concentration, the actual dye uptake per unit mass of adsorbent generally increases due to a stronger concentration gradient [43]. These results confirm that mustard waste-derived activated carbon is highly effective for the malachite green removal at lower concentrations. In comparison, higher concentrations may require a greater adsorbent dosage or an extended contact time to achieve enhanced treatment performance.

Adsorption kinetic studies: The kinetic behaviour of malachite green adsorption onto mustard waste-derived adsorbent was evaluated using pseudo-first-order (PFO), pseudo-second-order (PSO), Elovich and intraparticle diffusion (IPD) models. The corresponding kinetic parameters for these models, including PFO, PSO, Elovich and IPD, are summarised in Table-1 and their graphs are shown in Fig. 10, for malachite green dye concentrations ranging from 10 to 60 mg/L. The applicability of these models is assessed through the regression coefficient (R^2) values and the agreement between the experimental adsorption capacities ($q_{e,\,exp}$) and the calculated values ($q_{e,cal}$), which demonstrates the reliability of kinetic approach in describing the adsorption process. The pseudo-first-order model exhibited relatively low correlation coefficients (R^2 = 0.795-0.902) and calculated q_e values that deviated significantly from the experimental data, indicating that it was not suitable to describe the adsorption process. In contrast,

TABLE-1
ADSORPTION KINETIC PARAMETERS OF MALACHITE GREEN DYE ONTO MUSTARD WASTE-DERIVED ADSORBENT

Kinetics models	Parameters	Dye concentration (mg)					
		10	20	30	40	50	60
First order	q_e, exp	12.256	23.835	34.152	45.2	55.175	65.424
	K_1	0.0323	0.0272	0.0412	0.0313	0.0199	0.0286
	q_e, cal	6.463	10.59	14.81	22.77	20.61	29.53
	R	0.975	0.951	0.914	0.968	0.849	0.985
Second order	q_e, cal	13.55	26.06	36.76	49.72	59.84	71.78
	K_2	0.0069	0.0038	0.0039	0.0019	0.0016	0.0014
	R	0.997	0.996	0.998	0.997	0.995	0.997
Elovich	β	0.517	0.299	0.206	0.143	0.125	0.101
	α	11.22	39.5	66.9	46.06	72.05	78.2
	R	0.971	0.952	0.957	0.981	0.929	0.982
Intraparticle	K_{id}	0.642	1.127	1.548	2.312	2.659	3.252
	C	6.195	12.964	20.215	23.361	29.133	34.723
	R	0.988	0.983	0.934	0.993	0.945	0.994

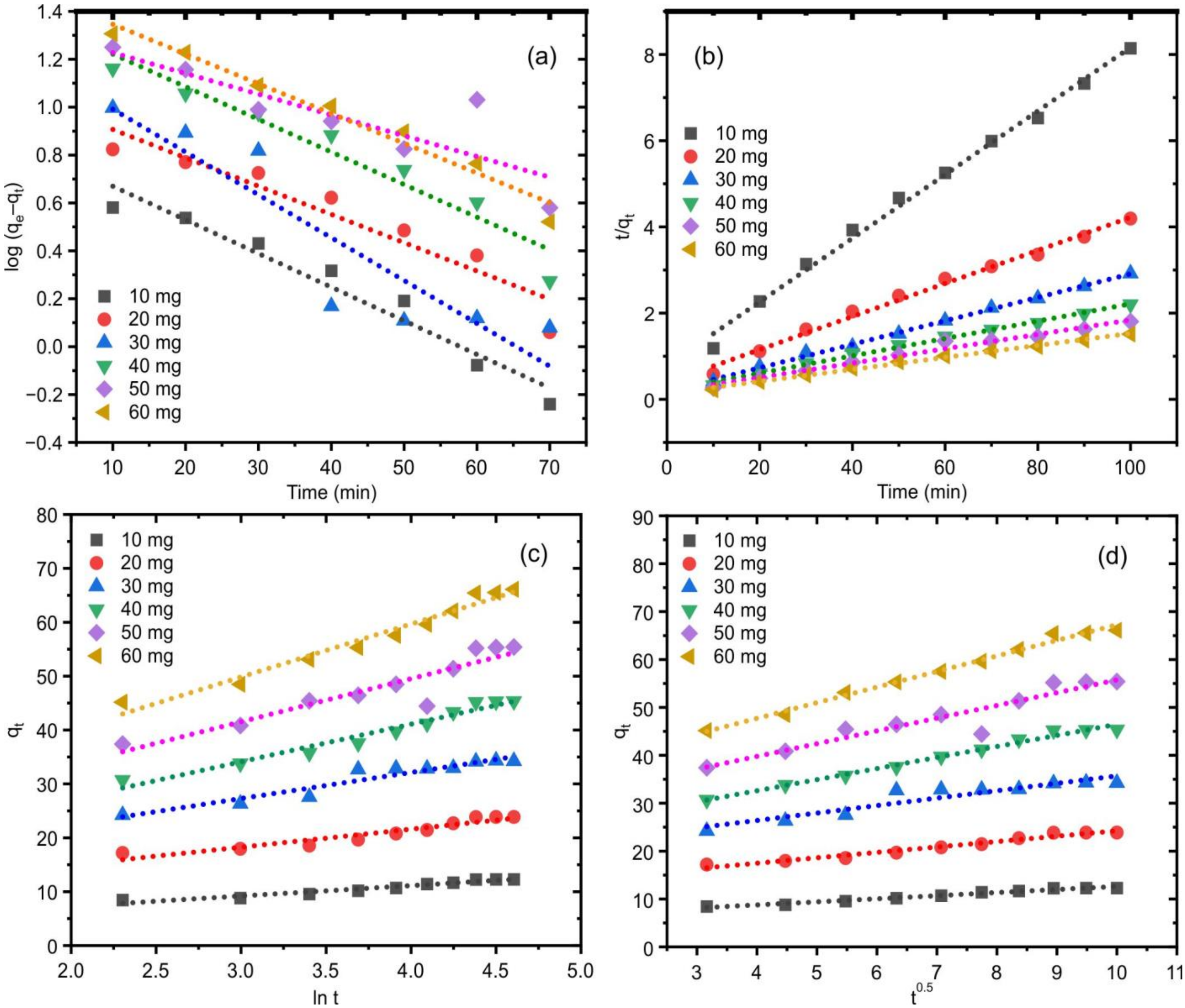

Fig. 10. Kinetic model fitting for the adsorption of malachite green dye onto mustard waste at different initial concentrations: (a) pseudo-first-order, (b) pseudo-second-order, (c) Elovich and (d) intraparticle diffusion models

the pseudo-second-order model provided an excellent fit with very high correlation coefficients (R^2 = 0.947-0.993) and calculated q_e values that closely matched the experimental ones across all dye concentrations. This confirms that the adsorption process follows a PSO kinetic model, suggesting that chemisorption, involving valence forces through electron sharing or exchange between adsorbent and adsorbate, is the dominant mechanism [44,45].

The Elovich model also showed good agreement (R^2 = 0.929-0.982), implying surface heterogeneity and a distribution of activation energies during adsorption. However, it was slightly less accurate than the second-order model. Furthermore, the intraparticle diffusion model indicated that dye uptake increased with higher initial concentrations, as reflected by the rising K_d values (0.642-3.252). However, the intercept ($C \neq 0$) suggests that intraparticle diffusion was not the sole rate-limiting step and boundary layer diffusion also contributed to the overall adsorption process [46-49].

Based on the kinetic studies, it is found that malachite green adsorption onto mustard waste-derived adsorbent is predominantly described by the pseudo-second-order model, indicating chemisorption as the principal rate-controlling mechanism, while the intraparticle diffusion contributes as a secondary transport process.

Adsorption equilibrium studies: The adsorption equilibrium data for the removal of malachite green onto mustard waste derived adsorbent was analysed using four isotherm models, namely Langmuir, Freundlich, Temkin and Dubinin–Radushkevich (D-R) [50]. Among these, the Langmuir model provided the best fit with a high correlation coefficient (R^2 = 0.987), indicating that the adsorption process predominantly follows monolayer coverage on a homogeneous surface. The maximum adsorption capacity (q_{max}) was determined to be 46.339 mg/g, suggesting that the adsorbent possesses a high affinity for malachite green dye. The Langmuir constant (b_L 0.469 L/mg) further supports the strong adsorbate–adsorbent interaction, while the separation factor value (R_L = 0.175), which lies between 0 and 1, confirms that the adsorption is highly favourable [51].

The Freundlich model also exhibited a strong correlation (R^2 = 0.985), reflecting the heterogeneous nature of the adsorbent surface. The Freundlich constant (K_F =19.436) indicated a considerable adsorption capacity and the value of the heterogeneity factor (n = 3.97 > 1) suggested that the adsorption process is favourable and primarily governed by the physical adsorption on a heterogeneous surface [52].

The Temkin model yielded a moderate fit (R^2 = 0.93), underscoring the influence of adsorbent-adsorbate interactions. The Temkin constant (B_T = 6.138 J/mol) suggests a mild heat of adsorption, which implies that the process involves both physisorption and weak chemisorption. Similarly, the D-R model showed the lowest correlation (R^2 = 0.75), with a mean adsorption energy value of E = 3.63 kJ/mol, which is below 8 kJ/mol, indicating that physical interactions predominantly govern the adsorption process [53,54].

The isotherm analysis indicates that malachite green dye adsorption onto mustard waste-derived adsorbent is favourable and efficient, with the Langmuir model providing the best fit for the equilibrium data. The findings (Fig. 11, Table-2) suggest that adsorption occurs predominantly through monolayer coverage, while surface heterogeneity also contributes to the uptake process. The mechanism is likely governed by a combination of physisorption with possible minor chemisorptive interactions.

Thermodynamics studies: The thermodynamic parameters governing the adsorption of malachite green dye onto mustard waste-derived adsorbent were evaluated and the results are shown in Table-3. By using the following equations, the thermodynamic parameters were evaluated:

$$\Delta G^o = -RT \ln K_C \quad (1)$$

$$\ln K_C = \frac{\Delta S^o}{R} - \frac{\Delta H^o}{RT} \quad (2)$$

where K_C is the equilibrium constant, T is the temperature in kelvin and R stands for the universal gas constant (8.314 J/mol K). According Table-3, the Gibbs free energy change (ΔG^o) values were negative at all studied temperatures, specifically at 293.15, 303.15 and 333.15 K. These negative ΔG^o values confirm the spontaneous nature of the adsorption

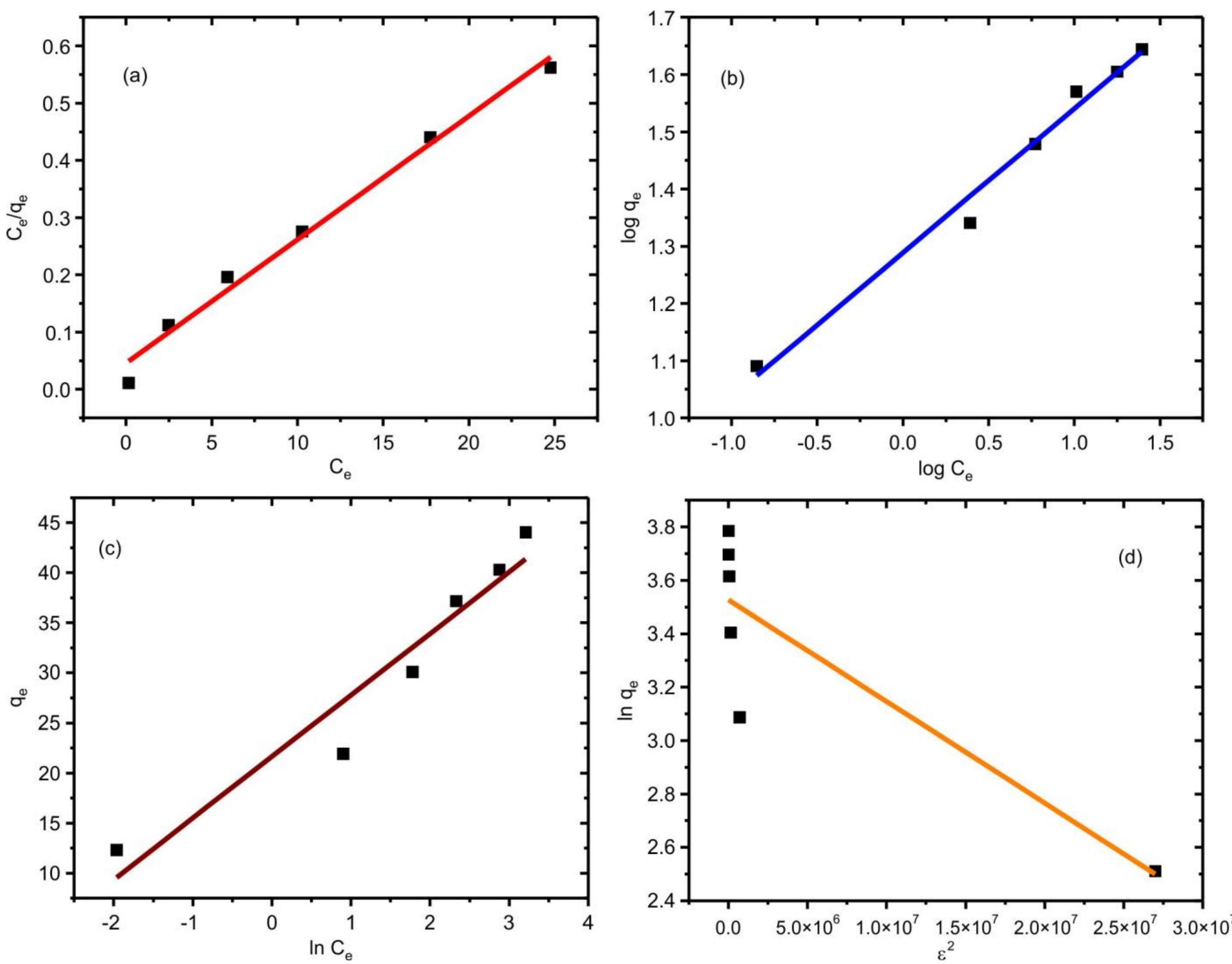

Fig. 11. Adsorption isotherm plots for malachite green removal using mustard waste derived adsorbent: (a) Langmuir, (b) Freundlich, (c) Temkin and (d) Dubinin–Radushkevich (D–R) models

TABLE-2
FITTED ISOTHERM MODEL PARAMETERS FOR MG DYE ADSORPTION ONTO MUSTARD WASTE DERIVED ADSORBENT

Isotherms	Parameters	Values of isotherm parameters
Langmuir	R^2	0.987
	q_{max}	46.339
	R_L	0.175
	b_L	0.469
Freundlich	R^2	0.985
	K_F	19.436
	n	3.97
Tempkin	R^2	0.93
	K_T	33.978
	B_T	6.138
	b_T	403.79
D-R	R^2	0.75
	K_{ad}	3.8×10^{-8}
	E	3625.09

TABLE-3
THERMODYNAMIC PARAMETERS ASSOCIATED WITH MALACHITE GREEN DYE ADSORPTION ON MUSTARD WASTE-DERIVED ADSORBENT

Temperature (K)	ΔG° (kJ mol^{-1})	ΔH° (kJ mol^{-1})	ΔS° (J mol^{-1} K^{-1})
293.15	-10.11		
303.15	-10.62	46.61	50.42
333.15	-12.13		

process, while the gradual decrease with increasing temperature indicates that higher temperatures favour malachite green uptake [55]. The positive enthalpy change (ΔH° = 46.61 kJ mol^{-1}) indicates the endothermic nature of adsorption, which is further supported by the improved dye removal at elevated temperatures. The positive entropy change (ΔS° = 50.42 J mol^{-1} K^{-1}) suggests increased randomness at the solid-liquid interface during adsorption, most likely due to the displacement of water molecules and structural adjustment in the adsorbent surface [56-58]. The van't Hoff plot (ln K_c *vs.* 1/T) exhibits a good linear relationship, validating the reliability of calculated parameters. Thus, the thermodynamic parameters indicate that malachite green adsorption onto a mustard waste-derived adsorbent is spontaneous, endothermic and entropy-driven, rendering the material highly suitable for practical dye removal applications.

Reusability: When assessing an adsorbent's long-term suitability and economic viability for wastewater treatment, reusability is a crucial factor. The current work used several adsorption-desorption cycles to examine the regeneration and reusability of activated carbon produced from mustard waste. To evaluate both recovery of adsorption performance and structural integrity over several cycles, the regeneration method involved desorbing malachite green from the spent adsorbent and then drying it before reuse.

The reusability of the prepared adsorbent was assessed through four successive adsorption-desorption cycles, as presented in Fig. 12. For reuse in malachite green adsorption, the exhausted adsorbent was regenerated by the solvent desorption method using an ethanol-water mixture as the eluent in batch mode. The regenerated mustard waste-derived

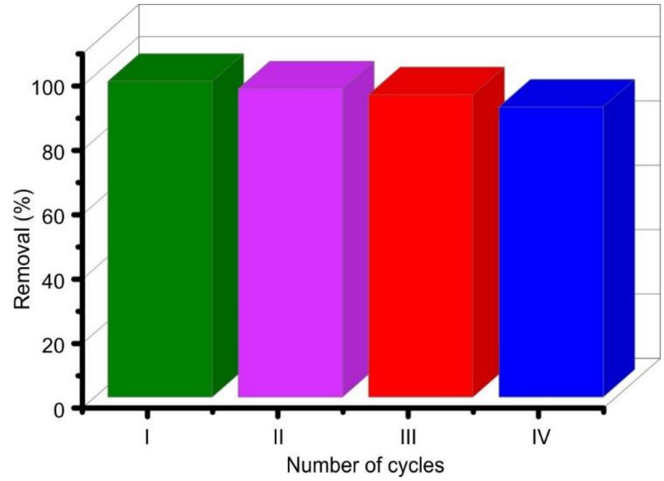

Fig. 12. Reusability of mustard waste-derived adsorbent for malachite green dye removal over four adsorption-desorption cycles

adsorbent was then applied to 200 mL of malachite green solution (30 mg/L) at pH 8 with an adsorbent dose of 0.1 g. Following adsorption, the spent material was again subjected to desorption and reused in subsequent cycles. In the first cycle, the removal efficiency was nearly 100%, indicating the excellent initial performance of the adsorbent. In the second and third cycles, only a slight decrease was observed. The gradual reduction in performance across cycles may be attributed to partial pore blockage or incomplete desorption of dye molecules. Nevertheless, the results confirm that the adsorbent exhibits excellent regeneration potential and can be effectively reused with minimal loss in adsorption efficiency, making it a promising candidate for sustainable and cost-effective wastewater treatment applications.

FT-IR analysis before and after adsorption: The FT-IR spectra of mustard waste-derived activated carbon before and after malachite green adsorption are shown in Fig. 13, revealing significant shifts and intensity changes in several characteristic bands. The broad band around 3400 cm^{-1} shifted following adsorption, clearly indicating the formation of hydrogen bonds between the amine groups of malachite green and the hydroxyl groups present in the lignocellulosic matrix of the adsorbent. Alterations observed in the 1600-1500 cm^{-1} region indicate π-π interactions between the aromatic rings and the lignin-derived aromatic structures of the activated carbon. Modifications in the C–N and C–O stretching regions (1400-1000 cm^{-1}) further demonstrate the participation of malachite green amine groups and oxygen-containing functional groups on the adsorbent surface in electrostatic interactions.

Furthermore, the reduced intensity of bands corresponding to –OH and C=O groups indicates their participation in the interaction with malachite green molecules. These spectral variations suggest that adsorption on the activated carbon surface involves specific chemical interactions alongside physical adsorption.

Comparative studies: For better comparison of adsorption performance, the efficiency of the mustard waste-derived activated carbon was evaluated alongside other low-cost adsorbents reported for malachite green removal (Table-4). The maximum adsorption capacity obtained in this study (46.34 mg g^{-1}) is in the same range as many agricultural waste–based

TABLE-4
COMPARISON OF ADSORPTION CAPACITIES FOR MALACHITE GREEN DYE USING LOW-COST ADSORBENTS

Adsorbent	Adsorbent source/activation	Maximum adsorption capacity, q_m (mg/g)	Isotherm model	Ref.
Fox nutshell activated carbon	$ZnCl_2$ activated agricultural waste	523.3	Langmuir	[59]
Okra stalk activated carbon	Microwave and chemical activated	119.05	Langmuir	[60]
Aegle marmelos-derived activated biochar	NaOH activated bael shell biochar	120.45	Langmuir	[61]
Aminated sal sawdust (ASSD)	Chemically modified sawdust	91.9	Langmuir	[62]
Rice husk	Raw rice husk agricultural waste	8.69	Langmuir	[63]
Mangosteen peel activated carbon	H_2SO_4 activated fruit peel	19.35	Langmuir	[64]
Mustard waste-derived activated carbon	KOH-activated mustard waste	46.34	Langmuir	Present study

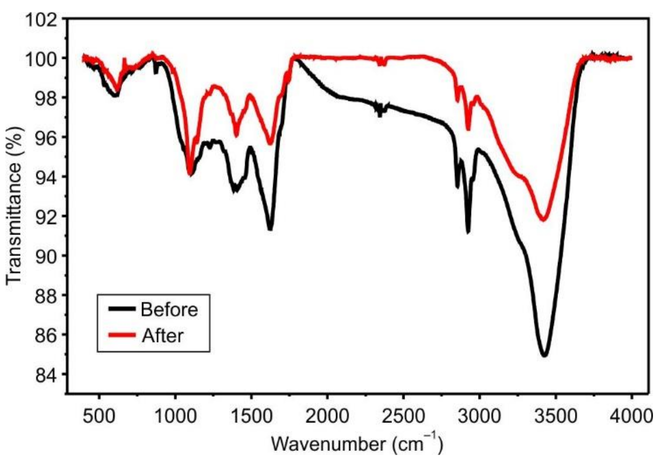

Fig. 13. FT-IR spectral analysis of mustard waste activated carbon before and after adsorption of malachite green dye

adsorbents described in previous studies. Although some chemically activated carbons show higher adsorption capacities, their preparation often involves more complex activation steps or the use of less sustainable raw materials. In contrast, the adsorbent developed in the present work provides a good balance between adsorption efficiency, low-cost precursor availability and a relatively simple preparation method. These characteristic features make it a promising material for practical wastewater treatment applications.

Conclusion

In this study, activated carbon derived from mustard waste was successfully synthesised and evaluated for the removal of malachite green dye from aqueous solutions. The prepared adsorbent exhibited high removal efficiency under optimised conditions, demonstrating its suitability as a low-cost and sustainable material for wastewater treatment. The equilibrium data were best fitted by the Langmuir isotherm model, indicating predominant monolayer adsorption, while the kinetic results followed the pseudo-second-order model, suggesting that the process is mainly governed by surface-controlled interactions. The adsorption of malachite green onto the prepared carbon is attributed to the combined influence of electrostatic attraction, pore filling and π-π interactions between the dye molecules and the functionalised carbon surface. This interpretation is supported by the pH-dependent adsorption behaviour, FTIR spectral changes and adsorption modelling studies. The regeneration experiments further showed that the adsorbent retained a substantial proportion of its adsorption capacity after repeated cycles, indicating good structural stability and reuse potential. These findings demonstrate that mustard waste can serve as an eco-friendly and economically viable precursor for activated carbon production. The study highlights the promise of agricultural waste-derived carbonaceous adsorbents for efficient treatment of dye-contaminated wastewater and supports the advancement of sustainable water purification technologies.

CONFLICT OF INTEREST

The authors declare that there is no conflict of interests regarding the publication of this article.

DECLARATION OF AI-ASSISTED TECHNOLOGIES

During the preparation of this manuscript, the authors used an AI-assisted tool(s) to improve the language. The authors reviewed and edited the content and take full responsibility for the published work.

REFERENCES

1. T.N. Lotha, V. Sorhie, P. Bharali and L. Jamir, *ChemistrySelect*, **9**, e202304093 (2024); https://doi.org/10.1002/slct.202304093
2. N. Nasuha and B.H. Hameed, *Chem. Eng. J.*, **166**, 783 (2011); https://doi.org/10.1016/j.cej.2010.11.012
3. S. Satyam and S. Patra, *Heliyon*, **10**, e29573 (2024); https://doi.org/10.1016/j.heliyon.2024.e29573
4. B. Senthil Rathi, P. Senthil Kumar, V. Kishore, S. Sridhar and G. Rangasamy, *Water Practice Technol*., **19**, 1849 (2024); https://doi.org/10.2166/wpt.2024.070
5. M.S. Soffian, F.Z.A. Halim, F. Aziz, M.A. Rahman, M.A.M. Amin and D.N.A.C. Awang, *Environ. Adv.*, **9**, 100259 (2022); https://doi.org/10.1016/j.envadv.2022.100259
6. D. Laishram, S.-B. Kim, S.-Y. Lee and S.-J. Park, *Adv. Sci.*, **12**, 2410383 (2025); https://doi.org/10.1002/advs.202410383
7. B. Kuppusamy, F.R.M. Ismail, P. Balakrishnan, S.-C. Kim, S.P. Asrafali and T. Periyasamy, *Polymers*, **18**, 180 (2026); https://doi.org/10.3390/polym18020180
8. B. Hu, Y. Ai, J. Jin, T. Hayat, A. Alsaedi, L. Zhuang and X. Wang, *Biochar*, **2**, 47 (2020); https://doi.org/10.1007/s42773-020-00044-4
9. Y. El maguana, N. Elhadiri, M. Benchanaa and R. Chikri, *J. Chem.*, **2020**, 2096834 (2020); https://doi.org/10.1155/2020/2096834
10. A.K. Meena, K. Kadirvelu, G.K. Mishraa, C. Rajagopal and P.N. Nagar, *J. Hazard. Mater.*, **150**, 619 (2008); https://doi.org/10.1016/j.jhazmat.2007.05.011
11. M. Haris, Z. Amjad, M. Usman, A. Saleem, A. Dyussenova, Z. Mahmood, K. Dina, J. Guo and W. Wang, *Biochar*, **6**, 47 (2024); https://doi.org/10.1007/s42773-024-00341-2

12. K. Intani, S. Latif, A.K.M.R. Kabir and J. Müller, *Bioresour. Technol.*, **218**, 541 (2016); https://doi.org/10.1016/j.biortech.2016.06.114
13. S. Charola, H. Patel, S. Chandna and S. Maiti, *J. Clean. Prod.*, **223**, 969 (2019); https://doi.org/10.1016/j.jclepro.2019.03.169
14. C.L. Zrybko, E.K. Fukuda and R.T. Rosen, *J. Chromatogr. A*, **767**, 43 (1997); https://doi.org/10.1016/S0021-9673(96)01068-0
15. M.S. Akindolie and H.J. Choi, *Environ. Eng. Res.*, **28**, 210574 (2023); https://doi.org/10.4491/eer.2021.574
16. T.F. Akinhanmi, E.A. Ofudje, A.I. Adeogun, P. Aina and I.M. Joseph, *Bioprocess*, **7**, 34 (2020); https://doi.org/10.1186/s40643-020-00325-0
17. Aruna, N. Bagotia, A.K. Sharma and S. Kumar, *Chemosphere*, **268**, 129309 (2021); https://doi.org/10.1016/j.chemosphere.2020.129309
18. Y. Zhao, X. Liu, W. Li, S. Pei, Y. Ren, X. Li, C. Qu, C. Wu and J. Liu, *Molecules*, **28**, 5310 (2023); https://doi.org/10.3390/molecules28145310
19. S.A. Alshareef, A.A. Alqadami, M.A. Khan, H.S. Alanazi, M.R. Siddiqui and B.-H. Jeon, *Bioresour. Technol.*, **347**, 126363 (2022); https://doi.org/10.1016/j.biortech.2021.126363
20. S. Hajati, M. Ghaedi and S. Yaghoubi, *J. Ind. Eng. Chem.*, **21**, 760 (2015); https://doi.org/10.1016/j.jiec.2014.04.009
21. S. Charola, H. Patel, S. Chandna and S. Maiti, *J. Clean. Prod.*, **246**, 969 (2019); https://doi.org/10.1016/j.jclepro.2019.03.169
22. S.S. Thakare, S.T. Shinde, R.S. Pawar, K.G. Sonawane and A.A. Kale, *Ceylon J. Sci.*, **54**, 945 (2025); https://doi.org/10.4038/cjs.v54i3.8549
23. Y. Shen, M. Ding, X. Ge and M. Chen, *Ind. Eng. Chem. Res.*, **54**, 8919 (2015); https://doi.org/10.1021/acs.iecr.5b02677
24. A.H. Wazir, I.U. Wazir and A.M. Wazir, *Energy Sources A Recovery Util. Environ. Effects*, **46**, 4875 (2020); https://doi.org/10.1080/15567036.2020.1715512
25. M. Demir, A.A. Farghaly, M.J. Decuir, M.M. Collinson and R.B. Gupta, *Mater. Chem. Phys.*, **216**, 508 (2018); https://doi.org/10.1016/j.matchemphys.2018.06.008
26. D. Angin, *Fuel*, **115**, 804 (2014); https://doi.org/10.1016/j.fuel.2013.04.060
27. U. Morali, H. Demiral and S. Sensoz, *J. Clean. Prod.*, **189**, 602 (2018); https://doi.org/10.1016/j.jclepro.2018.04.084
28. R.K. Liew, W.L. Nam, M.Y. Chong, X.Y. Phang, M.H. Su, P.N.Y. Yek, N.L. Ma, C.K. Cheng, C.T. Chong and S.S. Lam, *Process Saf. Environ. Prot.*, **115**, 57 (2018); https://doi.org/10.1016/j.psep.2017.10.005
29. X.-F. Tan, S.-S. Zhu, R.-P. Wang, Y.-D. Chen, P.-L. Show, F.-F. Zhang and S.-H. Ho, *Chinese Chem. Lett.*, **32**, 2939 (2021); https://doi.org/10.1016/j.cclet.2021.04.059
30. M. Makeswari and T. Santhi, *J. Water Resource Prot.*, **5**, 222 (2013); https://doi.org/10.4236/jwarp.2013.52023
31. M. Auta and B.H. Hameed, *Chem. Eng. J.*, **175**, 233 (2011); https://doi.org/10.1016/j.cej.2011.09.100
32. M. Patidar, S. Choudhary and R. Bhardwaj, *Mater. Today Proc.*, **47**, 6826 (2021); https://doi.org/10.1016/j.matpr.2021.05.139
33. C. Akmil-Başar, Y. Önal, T. Kılıçer and D. Eren, *J. Hazard. Mater.*, **127**, 73 (2005); https://doi.org/10.1016/j.jhazmat.2005.06.025
34. G.K. Gupta, P. Sagar, S.K. Pandey, M. Srivastava, A.K. Singh, J. Singh, A. Srivastava, S.K. Srivastava and A. Srivastava, *Nanoscale Res. Lett.*, **16**, 85 (2021); https://doi.org/10.1186/s11671-021-03545-8
35. M.A. Ahmad and R. Alrozi, *Chem. Eng. J.*, **171**, 510 (2011); https://doi.org/10.1016/j.cej.2011.04.018
36. M.A. Ahmad, N. Ahmad and O.S. Bello, *Water Air Soil Pollut.*, **225**, 2057 (2014); https://doi.org/10.1007/s11270-014-2057-z
37. S. Agarwal, I. Tyagi, V.K. Gupta, S. Mashhadi and M. Ghasemi, *J. Mol. Liq.*, **223**, 1340 (2016); https://doi.org/10.1016/j.molliq.2016.04.039
38. M. Yu, Y. Han, J. Li and L. Wang, *Chem. Eng. J.*, **317**, 493 (2017); https://doi.org/10.1016/j.cej.2017.02.105
39. Z. Chen, H. Deng, C. Chen, Y. Yang and H. Xu, *J. Environ. Health Sci. Eng.*, **12**, 63 (2014); https://doi.org/10.1186/2052-336X-12-63
40. N.M. Mahmoodi, B. Hayati, M. Arami and C. Lan, *Desalination*, **268**, 117 (2011); https://doi.org/10.1016/j.desal.2010.10.007
41. M. Alshabanat, R.S. Al-Mufarij and G.M. Al-Senani, *Orient. J. Chem.*, **32**, 3139 (2016); https://doi.org/10.13005/ojc/320636
42. M.N. Sepehr, A. Amrane, K.A. Karimaian, M. Zarrabi and H.R. Ghaffari, *J. Taiwan Inst. Chem. Eng.*, **45**, 635 (2014); https://doi.org/10.1016/j.jtice.2013.07.005
43. P.S. Kumar, S. Ramalingam, C. Senthamarai, M. Niranjanaa, P. Vijayalakshmi and S. Sivanesan, *Desalination*, **261**, 52 (2010); https://doi.org/10.1016/j.desal.2010.05.032
44. P. Kumari, K.M. Tripathi, K. Awasthi and R. Gupta, *Environ. Sci. Pollut. Res. Int.*, **30**, 15480 (2022); https://doi.org/10.1007/s11356-022-22883-3
45. P. Sharma, S. Sharma, S.K. Sharma, S. Yifei, F. Guo, T. Ichikawa, A. Jain and K. Shrivastava, *RSC Advances*, **14**, 29201 (2024); https://doi.org/10.1039/D4RA05442C
46. R. Sivashankar, A.B. Sathya, K. Vasantharaj and V. Sivasubramanian, *Environ. Nanotechnol. Monit. Manag.*, **1–2**, 36 (2014); https://doi.org/10.1016/j.enmm.2014.06.001
47. H. Chen and A. Wang, *J. Hazard. Mater.*, **165**, 223 (2009); https://doi.org/10.1016/j.jhazmat.2008.09.097
48. C.H. Weng, Y.T. Lin and T.W. Tzeng, *J. Hazard. Mater.*, **170**, 417 (2009); https://doi.org/10.1016/j.jhazmat.2009.04.080
49. P. Wang, Q. Ma, D. Hu and L. Wang, *React. Funct. Polym.*, **91–92**, 43 (2015); https://doi.org/10.1016/j.reactfunctpolym.2015.04.007
50. I. Rahman, B. Saad, S. Shaidan and E. Syarizal, *Bioresour. Technol.*, **96**, 1578 (2005); https://doi.org/10.1016/j.biortech.2004.12.015
51. S.A.H. Azaman, A. Afandi, B.H. Hameed and A.T. Mohd Din, *J. Appl. Sci. Engineering*, **21**, 317 (2018); https://doi.org/10.6180/jase.201809_21(3).0003
52. F. Amran, T. Sarawanan, Y.K. Qi, A. Azmi, A. Arsad and M.A.A. Zaini, *Int. J. Phytoremediation*, **27**, 36 (2025); https://doi.org/10.1080/15226514.2024.2399062
53. S.H. Tang and M.A.A. Ahmad Zaini, *J. Clean. Prod.*, **253**, 119970 (2020); https://doi.org/10.1016/j.jclepro.2020.119970
54. E. Akar, A. Altinisik and Y. Seki, *Ecol. Eng.*, **52**, 19 (2013); https://doi.org/10.1016/j.ecoleng.2012.12.032
55. A.K. Kushwaha, N. Gupta and M.C. Chattopadhyaya, *J. Saudi Chem. Soc.*, **18**, 200 (2014); https://doi.org/10.1016/j.jscs.2011.06.011
56. S. Azizian, S. Eris and L.D. Wilson, *Chem. Phys.*, **513**, 99 (2018); https://doi.org/10.1016/j.chemphys.2018.06.022
57. W. Qu, T. Yuan, G. Yin, S. Xu, Q. Zhang and H. Su, *Fuel*, **249**, 45 (2019); https://doi.org/10.1016/j.fuel.2019.03.058
58. S. Melhi, A.A. Alqadami, E.H. Alosaimi, G.M. Ibrahim, B. El-Gammal, M.A. Bedair and E.M. Elnaggar, *Water*, **16**, 1869 (2024); https://doi.org/10.3390/w16131869
59. A. Srivastava, R. Singh and N. Srivastava, *Indian J. Chem. Technol.*, **32**, 230 (2025); https://doi.org/10.56042/ijct.v32i2.11071
60. H. Yildiz, H. Gülşen, Ö. Şahin, O. Baytar and S. Kutluay, *Int. J. Phytoremediation*, **26**, 369 (2024); https://doi.org/10.1080/15226514.2023.2243621
61. A. Das, S. Roy, P.K. Saha and R.K. Jana, *Environ. Sci. Pollut. Res. Int.*, **31**, 15450 (2024); https://doi.org/10.1007/s11356-024-23890-3
62. P.L. Homagai, S. Rayamajhi, D. Dhami, R.L. Shrestha and D.P. Bhattarai, *Nepal J. Sci. Technol.*, **21**, 81 (2022); https://doi.org/10.3126/njst.v21i1.49917
63. N. Metin and S. Savcı, *Turkish J. Agric. Nat. Sci.*, **8**, 23 (2021); https://doi.org/10.30910/turkjans.749218
64. N.E. Yuningsih, L. Ariani, S. Suprapto, I. Ulfin, H. Harmami, H. Juwono and Y.L. Ni'mah, *J. Renew. Mater.*, **12**, 981 (2024); https://doi.org/10.32604/jrm.2024.049109